Effect of Cerium codoping on Er:BaY_2F_8 crystals

Elisa Sani, Alessandra Toncelli, Mauro Tonelli

NEST Dipartimento di Fisica, Università di Pisa, largo Pontecorvo, 3 - 56127 Pisa - Italy

sani@inoa.it

Abstract: We present the Erbium $^4I_{11/2}$ and $^4I_{13/2}$ complete polarized spectroscopic investigation on a series of Er^{3+},Ce^{3+}:BaY_2F_8 single crystals as a function of Cerium concentration. The main results of room temperature lifetime investigation show that the $^4I_{13/2}$ lifetime reduces from 15.6 ms to 10 ms, the $^4I_{11/2}$ lifetime reduces from 8.3 ms to 0.2 ms and $^4S_{3/2}$ lifetime reduces from 420 to 110 μs when adding 4% Ce-codoping. Moreover, in the same experimental conditions, the fluorescence intensity from $^4I_{13/2}$ increases by four times when adding 4%Ce, and the intensity of the 3 μm $^4I_{11/2} \rightarrow {}^4I_{13/2}$ transition becomes undetectable. The experimental data are interpreted with a rate equation model. The obtained results could be interesting in perspective of obtaining a low-threshold 1.5 μm Er laser.

OCIS codes: (160.3380) Laser materials; (160.5690) Rare earth doped materials; (140.3500) Lasers, erbium.

References and links

1. A. Agnesi, A. Guandalini, A. Lucca, E. Sani, A. Toncelli, M. Tonelli, D. Dell'Acqua "Medium-power diode-pumped Nd:BaY_2F_8 laser". Opt. Express **11**, 1149-1155 (2003), http://www.opticsexpress.org/abstract.cfm?URI=OPEX-11-10-1149
2. J.J. Zayhowski and J. Harrison, "Miniature solid-state lasers" in *Handbook of Photonics,* M.C. Gupta, ed. (CRC Press, Boca Raton, Fla., 1997)
3. W. Koechner, *Solid State Laser Engineering*, 5th edition, (Springer, Berlin, 1999)
4. A. A. Kaminskii, *Crystalline lasers: physical processes and operating schemes*, (CRC Press, Boca Raton, 1996).
5. H. J. Eichler, J. Findeisen, B. Liu, A. A. Kaminskii, A. V. Butachin, P. Peuser, "Highly efficient diode-pumped 3 μm Er^{3+}:BaY_2F_8 laser," IEEE J. Sel. Top. Quantum Electron. **3**, 90-94, (1997).
6. R. A. McFarlane, "Upconversion laser in BaY_2F_8:Er 5% pumped by ground-state and excited-state absorption," J. Opt. Soc. Am. B **11**, 871-880 (1994).
7. V.P.Gaponstev, S.M.Matitsin, A.A.Isyneev, V.B.Kravchenko, "Erbium glass lasers and their applications," Opt. Laser Technol. **14**, 189-196 (1982).
8. S. Jiang, J. Myers, D. Rhonehouse, M. Myers, R. Belford, S. Hamlin, "Laser and thermal performance of a new Erbium doped phosphate glass," Kigre, Hilton Head Island, 1990.
9. R. Fluck, U. Keller, E. Gini, H. Melchior, "Eyesafe pulsed microchip laser", OSA TOPS **19** Adv. Solid State Lasers, W.R. Bosenberg and M.M. Fejer eds. (OSA, Washington, DC 1998) 146-149.
10. P. Laporta, S. Longhi, S. Taccheo, O. Svelto, G. Sacchi, "Single-mode cw erbium-ytterbium glass laser at 1.5 μm," Opt. Lett. **18**, 31-33, (1993).
11. Choi Y G, Kim K H, Park S H, Heo J, "Comparative study of energy transfers from Er^{3+} to Ce^{3+} in tellurite and sulfide glasses under 980 nm excitation," J. Appl. Phys. **88**, 3832-3839, (2000).
12. Z. Meng,T. Yoshimura, K. Fukue, M. Higashihata, Y. Nakata, T. Okada, "Large improvement in quantum fluorescence yeld of Er^{3+}-doped fluorozirconate and fluoroindate glasses by Ce^{3+} codoping," J. Appl. Phys. **88**, 2187-2190, (2000).

#8713 - $15.00 USD Received 15 September 2005; revised 21 October 2005; accepted 21 October 2005

13. C. Strohofer, A. Polman, "Enhancement of Er^{3+} $^4I_{13/2}$ population in Y_2O_3 by energy transfer to Ce^{3+}," Opt. Mat. **17**, 445-451, (2001).
14. V.A.Lebedev, I.V.Voroshilov, B.V.Ignatiev, V.A. Isaev, A.N. Gavrilenko, V.F. Pisarenko, "Spectroscopic and kinetic investigations of erbium in Er,Ce:$CaGd_4Si_3O_{13}$ (Er,Ce:CGS) crystals," CLEO-Europe/EQEC, Techn. Digest, Paris, France, September 2000, paper CWF30.
15. E. Sani, A. Toncelli, M. Tonelli, D.A.Lis, E.V.Zharikov, K.A. Subbotin, V.A.Smirnov. "Effect of Cerium codoping in Er^{3+},Ce^{3+}:$NaLa(MoO_4)_2$ crystals," J. Appl. Phys. **97**, 123531, (2005).
16. B.Simondi-Teisseire, B.Viana, A.-M.Lejus, J. M. Benitez, D. Vivien, C. Borel, R. Templier,C. Wyon, "Room-temperature cw laser operation at ∼1.55 μm (eye-safe range) of Yb:Er and Yb:Er:Ce:$Ca_2Al_2SiO_7$ crystals," IEEE J. Quantum Electron. **32**, 2004-2009, (1996).
17. Y. Kubota, T. Teshima, N. Nishimura, S. Kanto, S. Sakaguchi, Z. Meng, Y. Nakata, and T. Okada, "Novel Er and Ce Codoped Fluoride Fiber Amplifier for Low-Noise and High-Efficient Operation With 980-nm Pumping," IEEE Photonics Technol. Lett., **15**, 525-527 (2003).
18. Y. Akasaka, Y. Kubota, S. Sakaguchi, I. White and J. Pan,"100 nm gain bandwidth amplifier based on 980 nm pumped cerium codoped fluoride EDF," Electron. Lett. **39**, 836-838 (2003).
19. S. Guy, M. F. Joubert, B. Jacquier, M. Bouazaoui, "Excited-state absorption in BaY_2F_8:Nd^{3+}," Phys. Rev. B **47**, 11001-6 (1993).
20. D. S. Knowles, H. P. Jenssen, "Upconversion versus Pr-deactivation for efficient 3 μm laser operation in Er," IEEE J. Quantum Electron. **28**, 1197-1208, (1992).
21. G. A. Kumar, R. Riman, S. C. Chae, Y. N. Jang, I. K. Bae, H. S. Moon, "Synthesis and spectroscopic characterization of CaF_2:Er^{3+} single crystal for highly efficient 1.53 μm amplification," J. Appl. Phys. **95**, 3243-49, (2004).
22. J. C. Brice, *The growth of crystals from liquids*, (North-Holland, Amsterdam, 1973)
23. B. F. Aull, and H. P. Jenssen, "Vibronic interactions in Nd:YAG resulting in nonreciprocity of absorption and stimulated emission cross sections," IEEE J. Quantum Electron. **18**, 925, (1982).

1. Introduction

Despite the considerable amount of work on laser emission from Er-doped crystals, the laser characteristics of the 1.5 μm $^4I_{13/2} \rightarrow {}^4I_{15/2}$ ground state transition are rather poor. The intrinsic difficulty to obtain laser action on this transition is mainly related to its three-level characteristic, but also other effects have to be taken into account like for example the poor feeding efficiency when pumping into the $^4I_{11/2}$ level, and the upconversion process that depopulates the $^4I_{13/2}$ multiplet.

Fluoride hosts are characterized by lower phonon energy than oxides. That increases the probability of radiative infrared transitions. Among fluorides, BaY_2F_8 (BaYF) is a very attractive material thanks to its good thermomechanical properties. In fact, it has a thermal conductivity (∼ 0.06 W/cmC [1]) comparable to that of YVO_4 (0.05 W/cmC [2]), moreover its non-cubic structure can compensate the thermal lens under strong pumping as it happens in $LiYF_4$, rather then in cubic crystals such as YAG [3]. In particular, BaYF appears interesting for the development of a 1.5 μm Er laser because it provides a larger Stark splitting for rare earth energy levels than other fluorides do, allowing good efficiency even for three-level lasers [4].

The Er doping of BaYF has already been investigated as for efficient laser emission at 3 μm [5] or in the green-blue region [6]. To the best of our knowledge, 1.5 μm laser emission in BaYF has been reported only once in [6], where the authors incidentally obtained IR emission while studying the dependence of the blue laser on the pump wavelength. No further efforts have been made up to now to characterize the 1.5 μm laser in this crystal.

Because of the fact that an efficient 1.5 μm Er^{3+} laser oscillation has been demonstrated only in some Erbium-doped glasses so far [7]-[10], to improve the efficiency of population inversion at 1.5 μm, codoping with Cerium has been investigated in some vitreous [11] [12] and crystalline materials [13]-[16] and it has even proved to increase the amplification efficiency in some Er-doped fiber amplifiers[17] [18].

#8713 - $15.00 USD Received 15 September 2005; revised 21 October 2005; accepted 21 October 2005

The aim of the present work is to study the effects of Erbium-Cerium codoping in BaYF fluoride host. To this aim, we grew several Er-Ce:BaYF crystals, doped with the same nominal amount of Erbium and different Cerium concentrations and we characterized them as for the Er 1.5 μm emission.

2. Crystal structure and Er-Ce energy transfer in fluorides

BaYF has monoclinic structure and the rare earth dopants enter substitutionally the Y^{3+} sites [19]. It is isostructural to $BaEr_2F_8$, so that it can be doped up to 100% Er while maintaining the same structure. On the other hand Ce^{3+} ion has an ionic radius larger than Y^{3+}, therefore the Ce doping introduces a considerable stress in the crystalline matrix. Moreover, unlike Er, Cerium does not have a compound analogous to $BaEr_2F_8$. For both reasons, an high Ce doping level in BaYF is not possible.

Due to the complex nature of the Erbium energy level scheme, many processes have to be taken into account when investigating its laser characteristics (see for example [20]). A possible approach to help the population inversion is to deactivate the detrimental level(s) through energy transfer to another rare earth. This approach has successfully been tried in the case of Er 3 μm laser, using Pr as deactivator [20], that effectively depopulates the $^4I_{13/2}$ multiplet and leaves the $^4I_{11/2}$ lifetime unchanged.

Codoping with Ce has been investigated in the present work in order to selectively quench the $^4I_{11/2}$ lifetime instead. Ce has only one electron in the *4f* orbital, therefore it has only one excited energy level in the *4f* configuration, with an energy about 3000 cm^{-1} higher than the ground state. Therefore it is quickly depopulated by strong multiphonon decay at room temperature. The next excited state of Ce is a *5d* configuration state. In fluorides, the transition to the ground state is situated in the UV region of the spectrum. Moreover this transition is electric-dipole allowed, leading to lifetimes as short as few nanoseconds.

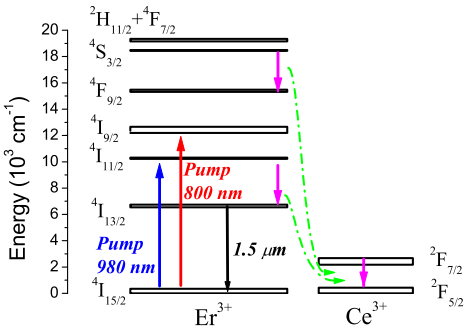

Fig. 1. Schematics of the Er-Ce energy transfer processes in BaYF.

Before giving the processes involved in the case of Er-Ce codoped fluoride systems in some detail, it is first important to notice that, since Ce does not absorb the radiation used to pump Er (except UV radiation), it will not adversely affect the pumping efficiency under diode pumped operation. The processes involved in energy transfer in Er-Ce codoped systems, at low (1%) Er concentrations, are shown in Fig. 1. In agreement with the literature, Ce is assumed to primarily increase the $^4I_{11/2} \rightarrow ^4I_{13/2}$

#8713 - $15.00 USD Received 15 September 2005; revised 21 October 2005; accepted 21 October 2005

branching ratio, according to the following path:

$$^4I_{11/2}(Er),^2F_{5/2}(Ce) \rightarrow ^4I_{13/2}(Er),^2F_{7/2}(Ce) \quad (1)$$

As the energy difference between the two Er levels is about 3700 cm^{-1}, whereas the energy difference between the two lower levels of Ce is about 3000 cm^{-1}, it is reasonable that the process involves one Ce ion and two lattice phonons.

The $^4S_{3/2}$ level in fluorides is populated mainly by upconversion from the long-living $^4I_{11/2}$. Therefore, the depopulation of this latter level also reduces the amount of pump energy that is lost via upconversion. Moreover, by looking at the energy gap between $^4S_{3/2}$ and $^4F_{9/2}$ (about 3000 cm^{-1}) we could also infer a further direct quenching of $^4S_{3/2}$ by Cerium, according to the scheme:

$$^4S_{3/2}(Er),^2F_{5/2}(Ce) \rightarrow ^4F_{9/2}(Er),^2F_{7/2}(Ce) \quad (2)$$

In addition, the energy gap between the $^4F_{9/2}$ and $^4I_{9/2}$ multiplets is also consistent with the Ce upper *4f* to ground state energy difference, and therefore it seems reasonable to expect also a $^4F_{9/2}$ quenching by Cerium as follows:

$$^4F_{9/2}(Er),^2F_{5/2}(Ce) \rightarrow ^4I_{9/2}(Er),^2F_{7/2}(Ce) \quad (3)$$

As a result Ce codoping can give rise to a series of cascade quenching processes which accumulates the energy on the $^4I_{13/2}$ 1.5 μm-emitting level. The cascade quenching stops on the $^4I_{13/2}$, because the energy gap from this level to the ground state (about 6600 cm^{-1}) is much higher than the energy separation between the two levels of Ce.

3. Experimental

BaYF single crystals, doped with 1% Er concentration and with different amounts of Ce have been grown by the Czochralski method from oriented seeds. The growth parameters were: temperature around 970 °C, pull rate 0.5 mm/h, rotation rate 10 RPM. We grew a total of five samples, with Ce concentrations of 0%, 0.2%, 0.5%, 2% and 4% in the melt. As the ionic radius of Ce is larger than that of Y, the optical quality of the samples tends to degrade with Ce concentration. For this reason the maximum investigated doping level is 4%Ce,1%Er:BaYF which was still of reasonably good optical quality.

All the crystals were oriented by X-ray backscattering Laue diffractometry and cut with edges parallel to the *b* and *c* crystallographic axes in order to investigate polarization-dependent optical properties.

The polarized absorption spectra were performed at room temperature, with a Cary 500 spectrophotometer.

We recorded the emission spectra around 500 nm ($^4S_{3/2} \rightarrow ^4I_{15/2}$ transition), 1.5 μm ($^4I_{13/2} \rightarrow ^4I_{15/2}$ transition) and 3 μm ($^4I_{11/2} \rightarrow ^4I_{13/2}$ transition). The excitation source was a 150-mW diode laser tuned at 968 nm. The luminescence was observed perpendicularly to the exciting beam to avoid pump spurious scattering. It was mechanically chopped and focused by a lens of 75 mm focal length on the input slit of a 25-cm monochromator equipped with a 1200 gr/mm, a 600 gr/mm or a 300 gr/mm grating for the different investigated wavelength regions and filtered by a Si or by a Ge window in the case of 1.5 μm or 3 μm measurements, respectively. The signal was detected by a S20 photomultiplier for the green region or by a cooled InSb detector in the infrared and processed by a lock-in amplifier. The resolution of the fluorescence spectra was 4.5 nm in the visible region, 3 nm at 1.5 μm and 24 nm at 3 μm.

#8713 - $15.00 USD Received 15 September 2005; revised 21 October 2005; accepted 21 October 2005

In order to evaluate the 1.5 μm Er emission cross sections we acquired the polarized emission spectra at room temperature on the singly-doped sample. In this case the excitation source was a diode array delivering up to 2 W at 968 nm. The fluorescence was dispersed by a 32-cm monochromator, equipped with a 600 gr/mm grating. Also in this case the detector was a cooled InSb photodiode. The resolution of the polarized 1.5 μm emission spectra was 1 nm.

For the $^4I_{11/2}$ and $^4I_{13/2}$ multiplets lifetime measurements we used a pulsed tunable Ti:Al_2O_3 laser with 10 Hz repetition rate and 20 ns pulse width as a source. The laser was tuned to the peak of the $^4I_{15/2} \rightarrow ^4I_{9/2}$ absorption band, at 794 nm. To better characterize the Er-Ce energy transfer dynamics, we also measured the green-emitting $^4S_{3/2}$ level lifetime. In this case the excitation source was the pulsed Ti:Al_2O_3, doubled by a BBO crystal. The excitation wavelength was 407 nm. In all lifetime measurements, the pulse energy was reduced as much as possible in order to minimize power-dependent effects. The fluorescence was collected from a short portion of the sample to observe a uniformly pumped volume. To reduce the spurious decaytime lengthening produced by radiation trapping the laser was focussed at the edge where the observation was made. Detection of the laser scattering was avoided by means of suitable filters. The signal was detected by a cooled InSb detector for the infrared cases and by a S20 photomutiplier for the visible region and was sent, after amplification, to a digital oscilloscope connected to a computer. The response time of the system was about 1 μsec.

4. Spectroscopy

Preliminary unpolarized absorption measurements have been performed for every crystal from 187 nm up to 3 μm, over the whole operating range of the spectrophotometer, in order to check the presence of unwanted contaminants. The recorded spectra allow us to infer that the crystals are free of OH^- radicals or other impurities within the sensitivity of our instrument.

In Fig. 2 the Cerium absorption spectrum, of the sample doped with 1% Er and 0.2% Ce, is shown. Because of the very high Ce absorption, the measurements have been performed on samples less than 1 mm thick. The band around 200 nm is relative to the transition $^2F_{5/2} \rightarrow ^2D_{5/2}$ (the third peak at the shortest wavelength is missing because it lies out of the operating range of the spectrophotometer). The remaining peaks are centered at 246 nm and 301 nm and can be assigned to the $^2F_{5/2} \rightarrow ^2D_{3/2}$ transition. The first one shows a shoulder at 255 nm that can be ascribed to Er $^4I_{15/2} \rightarrow ^4D_{7/2}$. The spectra of the samples with different Ce doping level have identical shapes, but their intensities are different.

The polarized absorption spectrum of the Er $^4I_{15/2} \rightarrow ^4I_{11/2}$ transition at room temperature is shown in Fig. 3. This band has been used for diode pumping. The peak values are $\alpha = 1$ cm^{-1} at 968 nm in $\mathbf{E}||\mathbf{b}$ polarization, and 0.8 cm^{-1} at 970 nm for $\mathbf{E}||\mathbf{c}$, and are the same for all the samples showing that the Er doping level does not change.

The comparison of the emission spectra intensities at 1.5 μm is shown in Fig. 4 for all the samples except the 0.5%-Ce codoped one, because its emission spectrum was almost undistinguishable from that obtained in case of 0.2%-Ce codoping. The samples were compared in the same geometrical conditions, by using a specially designed mount to reproduce the same experimental conditions in all cases. The intensity increases with the Ce content in the crystals, and in the most heavily Ce-doped one it is five times larger than in the case of solely-Er doped sample.

A confirmation of the quenching effect of Ce is given by the intensity trend of the $^4I_{11/2} \rightarrow ^4I_{13/2}$ Er transition. We obtained that the 3 μm fluorescence intensity mono-

#8713 - $15.00 USD Received 15 September 2005; revised 21 October 2005; accepted 21 October 2005

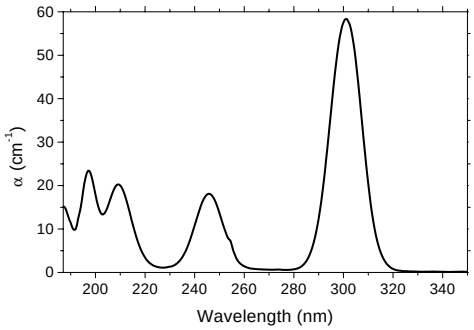

Fig. 2. Unpolarized absorption spectrum of the sample with the 0.2% Ce concentration.

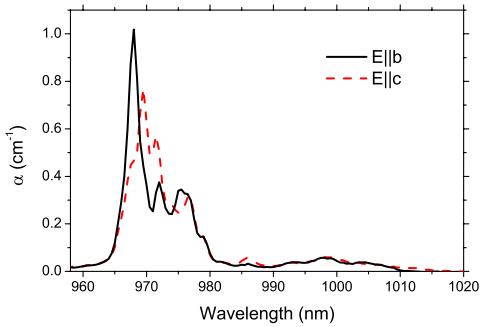

Fig. 3. Polarized absorption spectrum of the $^4I_{15/2} \rightarrow ^4I_{11/2}$ transition of Er.

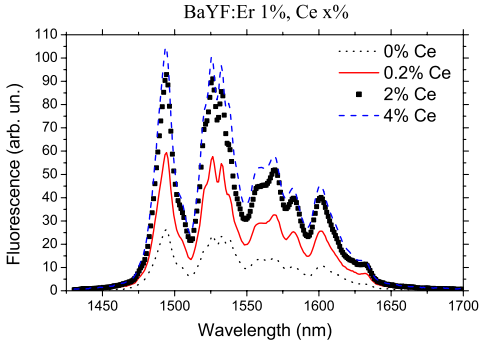

Fig. 4. $\mathbf{E} \perp \mathbf{c}$ emission spectrum of the $^4I_{13/2} \rightarrow ^4I_{15/2}$ transition of Er.

#8713 - $15.00 USD Received 15 September 2005; revised 21 October 2005; accepted 21 October 2005

tonically decreases with increasing Ce concentration (the opposite of the $^4I_{13/2} \rightarrow ^4I_{15/2}$ intensity trend). For the sample codoped with 2% Ce, the intensity reduces to about 10% with respect to the solely-Er doped crystal. For the 4% Ce codoped sample, the 3 μm emission is undetectable.

The room temperature lifetimes of the $^4I_{11/2}$ and $^4I_{13/2}$ multiplets of Erbium are summarized in Table 1. The $^4I_{13/2}$ lifetimes are exponential in all the samples, whereas the $^4I_{11/2}$ ones are exponential only in the samples doped with 0%, 0.2% and 0.5% Ce. In the two higher-Ce concentration crystals these decays are markedly non-exponential giving evidence of a strong quenching of this level by Ce. For a uniform evaluation of the lifetimes both in exponential and non-exponential cases, all the values in Table 1 have been calculated as the integral of the decay curve normalized to the initial intensity. The given lifetime values have been calculated as average of the value of the normalized decay integrals in a series of different subsequent acquisitions, whereas the uncertainties have been evaluated as the standard deviation of the same measurements series.

Our results show that in the sample doped only with Er the decaytime of the upper level is about half of that of the lower one. The Cerium presence selectively shortens the $^4I_{11/2}$ lifetime, and in the 4% Ce codoped sample the ratio of the lifetimes of the $^4I_{11/2}$ and $^4I_{13/2}$ levels reduces to about a fiftieth. The lifetime characteristics and the 3 μm intensity trend are a clear indication of the Ce effect in depopulating the Er $^4I_{11/2}$ level and in feeding the $^4I_{13/2}$ multiplet. Moreover the behavior of the 1.5 μm emission intensity confirms this hypothesis even if the lifetime dependence of this level suggests that a slight quenching effect takes place on this level, too. Anyway in this case the intensity of the quenching is much smaller than on the other excited levels, probably thanks to the worse energy matching of the gaps involved. This is clear from three main facts: first the lifetime shortening is less pronounced, secondly the decay behavior is always exponential, and finally the intensity of the emission increases with Ce concentration.

Table 1. Erbium lifetimes as a function of the Cerium codoping.

sample	lifetime $^4I_{13/2}$ (ms)	lifetime $^4I_{11/2}$ (ms)
1% Er	15.6 ± 0.5	8.3 ± 0.2
1% Er -0.2% Ce	13.6 ± 0.4	6.7 ± 0.3
1% Er -0.5% Ce	12.4 ± 0.4	5.1 ± 0.1
1% Er-2% Ce	10.5 ± 0.3	1.98 ± 0.04
1% Er-4% Ce	10.3 ± 0.3	0.23 ± 0.01

To fully characterize the Er-Ce:BaYF system, we also analyzed the $^4S_{3/2} \rightarrow ^4I_{13/2}$ transition, because in case of diode pumping on the 970-nm band, upconversion population of the $^4S_{3/2}$ green-emitting multiplet is also detrimental to feeding $^4I_{13/2}$. In fact, one of the most important loss channels for the $^4I_{13/2}$ population is due to parasitic pop-

#8713 - $15.00 USD Received 15 September 2005; revised 21 October 2005; accepted 21 October 2005

ulation of the high-lying levels. We found that the intensity of the green fluorescence dramatically decreases in the Ce-codoped samples (it reduces by about a hundred times when adding 4% Ce). This is related both to the depopulation of the $^4I_{11/2}$ level and to a direct cascade quenching of the $^4S_{3/2}$ by Cerium and it increases the efficiency of the 980 nm pumping, allowing the energy of the pump to be mainly deposed on the upper 1.5 μm level. In Fig. 5 the intensity trends of the $^4I_{13/2} \rightarrow ^4I_{15/2}$ (black squares) and the $^4S_{3/2} \rightarrow ^4I_{15/2}$ (red triangles) transitions as a function of the Ce concentration are shown together. As we can see, the effect tends to saturate at the highest Ce concentrations we studied.

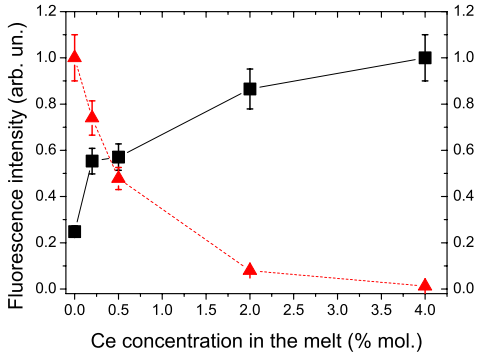

Fig. 5. Comparison of the normalized emission intensities as a function of the Ce concentration: black squares: 1.5 μm transition; red triangles: $^4S_{3/2}$ transition.

To characterize the direct quenching of the Er $^4S_{3/2}$ by Ce, we measured the lifetime of this level under blue excitation into the $^2H_{11/2}$ level, which can be practically considered as a direct $^4S_{3/2}$ excitation because of the thermal coupling of these two manifolds at room temperature. The decays are not exponential, except for the case of the sample doped only with Er, therefore we calculated the integral of the decay curve normalized to its initial intensity as an estimate of the effective lifetime. In Table 2 the integral lifetimes are listed. Similarly to the $^4I_{11/2}$ and $^4I_{13/2}$ cases, the values of the lifetimes and of their respective uncertainties we give in Table 2 arise from the average and the standard deviation we calculated on a series of following measurements. The $^4S_{3/2}$ lifetime reduces to a fourth in the 4% Ce-codoped sample, compared to the solely-Er doped one. This is a clear indication that a direct quenching of the $^4S_{3/2}$ multiplet by Ce also takes place (Eq. 2) and, accordingly, a further quenching of the $^4F_{9/2}$ (Eq. 3) is likely.

As we can see, the Ce codoping in Er-doped BaYF produces two effects: first, a cascade quenching for all the excited energy levels which is larger the smaller their energy gap. Therefore this quenching effect is expected to be maximum for the $^4S_{3/2}$, $^4F_{9/2}$ and $^4I_{11/2}$ multiplets because their energy gaps are close to that of Ce, and minimum for the $^4I_{13/2}$, whose energy gap is by far the largest. The second effect of Ce is that the depopulation of all the energy levels lying above $^4I_{13/2}$ (in particular $^4I_{11/2}$) quenches the upconversion mechanisms towards the high-lying levels. Both these effects improve the population efficiency of the $^4I_{13/2}$ and make the population inversion for the 1.5 μm laser easier.

#8713 - $15.00 USD Received 15 September 2005; revised 21 October 2005; accepted 21 October 2005

Table 2. Erbium $^4S_{3/2}$ lifetimes as a function of the Cerium codoping.

sample	$^4S_{3/2}$ lifetime (μs)
1% Er	421 ± 2
1% Er -0.2% Ce	381 ± 4
1% Er -0.5% Ce	364 ± 1
1% Er-2% Ce	277 ± 4
1% Er-4% Ce	107 ± 1

5. Laser parameters

Erbium emission cross sections at 1.5 μm have been calculated by the integral β-τ method [23], using the polarized room-temperature emission spectra and the measured value of the $^4I_{13/2}$ lifetime in the case of the sample without Ce. Because of the magnetic-dipole contribution to the $^4I_{13/2} \rightarrow {}^4I_{15/2}$ transition and the monoclinic symmetry of the crystal, we considered the total of the six different polarizations allowed by both the electric and magnetic field directions. In Fig. 6 we show three polarizations only, for clarity. The shape of the obtained cross section curves is strongly dependent on the polarization, the peak values are $6.3 \cdot 10^{-21}$, $10.3 \cdot 10^{-21}$ and $4.5 \cdot 10^{-21}$ cm^2 at 1538 nm in the (**E**||**c** & **H**||**c**), (**E**||**c** & **H**||**b**) and (**E**⊥**b,c** & **H**||**c**) polarizations, respectively.

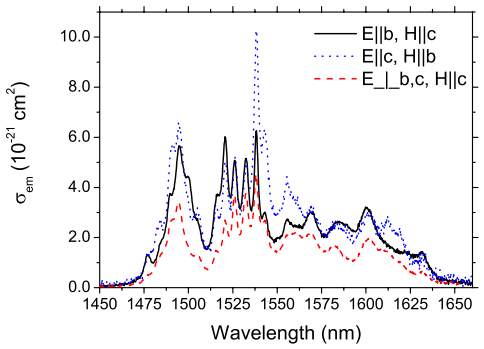

Fig. 6. Polarized Erbium emission cross sections.

An evaluation of the laser gain as a function of the inversion coefficient γ (defined as the ratio of the population of the upper laser level over the total Er^{3+} upper and lower level population densities) is possible by using the formula:

$$\sigma_{gain}(\lambda) = \gamma\sigma_{em}(\lambda) - (1-\gamma)\sigma_{abs}(\lambda) \tag{4}$$

#8713 - $15.00 USD Received 15 September 2005; revised 21 October 2005; accepted 21 October 2005

where σ_{em} labels the emission cross section and σ_{abs} the absorption one. In Fig. 7 we show the gain cross section for different values of the γ parameter, for the (**E**||**b** & **H**||**c**) polarization. From the Fig. 7, we are able to estimate the most probable lasing wavelength in this polarization to be around 1615 nm, with a net gain region from 1601.3 to 1625.8 nm for $\gamma = 0.2$, and from 1536.7 to about 1640 nm if $\gamma = 0.4$.

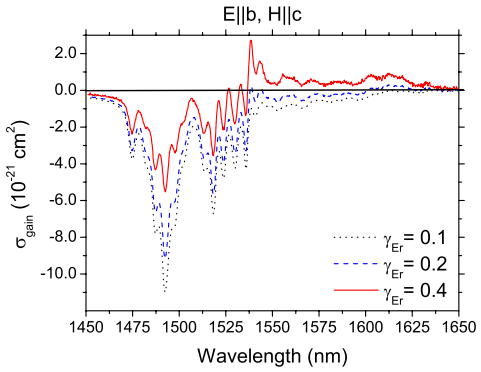

Fig. 7. Gain cross section in the E||b, H||c polarization of Er:BaYF.

In order to quantitatively evaluate the Ce effect on the feeding efficiency of the $^4I_{13/2}$ Er multiplet, we developed a simplified "three-plus-one-level" model (Fig. 8), in which the Ce effect is modelized with a β_{Ce} parameter which takes into account the $^4I_{11/2}$ lifetime shortening. The decreasing of the $^4I_{13/2}$ lifetime is phenomenologically considered by using in the calculations the measured value for every crystal. It is important to underline that our model neglects all upconversion mechanisms. Therefore its validity increases as a function of the Ce concentration in the samples (for fixed pump power) because of the Ce effect that decreases the upconversion processes.

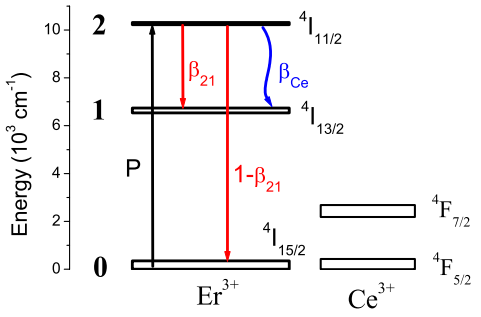

Fig. 8. Schematics of the model used for Eqs. 5-8.

In case of pure Er doping, the system (neglecting upconversion) is characterized by

#8713 - $15.00 USD Received 15 September 2005; revised 21 October 2005; accepted 21 October 2005

the following set of coupled rate equations:

$$\begin{cases} \frac{dN_2}{dt} = PN_0 - \frac{N_2}{\tau_2} & (a) \\ \frac{dN_1}{dt} = \beta_{21} \cdot \frac{N_2}{\tau_2} - \frac{N_1}{\tau_1} & (b) \\ N_2 + N_1 + N_0 = N_{Er} & (c) \end{cases} \tag{5}$$

where N_2, N_1 and N_0 are the populations of the $^4I_{11/2}$, $^4I_{13/2}$ and $^4I_{15/2}$ levels, respectively, and N_{Er} is the Er doping density. P is the pump rate (expressed as absorbed photons per unit time). τ_2 and τ_1 are the measured lifetimes of the 2 and 1 multiplets, respectively, in the solely-Er-doped crystal.

We can explicitly write the inversion coefficient γ of Eq. 4 as:

$$\gamma = \frac{N_1}{N_1 + N_0} \tag{6}$$

In the following, the γ parameter for the crystal without Ce will be indicated as γ_{Er}, whereas γ_{Er-Ce} will indicate the parameter in case of Er-Ce codoped systems. When needed for a clear identification of the crystal we will speak about, the concentration of Ce will be explicitly written (for instance $\gamma_{Er-2\%Ce}$).

By considering the stationary case, from Eqs. $5(a)-(c)$ we obtain the following relation between the γ_{Er} parameter and the pump rate P:

$$P = \frac{1}{\tau_1 \beta_{21}} \cdot \frac{\gamma_{Er}}{1 - \gamma_{Er}} \tag{7}$$

In case of Er-Ce codoping, the rate equations become:

$$\begin{cases} \frac{dN_2}{dt} = PN_0 - \frac{N_2}{\tau_2} - \beta_{Ce} \cdot \frac{N_2}{\tau_2} & (a) \\ \frac{dN_1}{dt} = \beta_{21} \cdot \frac{N_2}{\tau_2} + \beta_{Ce} \cdot \frac{N_2}{\tau_2} - \frac{N_1}{\tau_1^*} & (b) \\ N_2 + N_1 + N_0 = N_{Er} & (c) \end{cases} \tag{8}$$

where β_{Ce} is connected to the measured value τ_2^* of the $^4I_{11/2}$ lifetime in the sample under investigation by the following equation:

$$\frac{1}{\tau_2} + \frac{\beta_{Ce}}{\tau_2} = \frac{1}{\tau_2^*} \tag{9}$$

which models the cross-relaxation of Eq. 1 as a linear decay. This model is correct only if the ground state population of Ce is constant, as it seems reasonable to expect given the strong multiphonon relaxation at room temperature of the Ce $^3F_{7/2}$. Moreover, from a rate equation analysis we found that the Er $^4I_{11/2}$ population is always much smaller than the Ce ground state population for every Ce concentration. This ensures that the Ce quenching is always effective.

In Eqs. $8(a)-(c)$ N_2, N_1, N_0 and N_{Er} are the populations of the $^4I_{11/2}$, $^4I_{13/2}$ and $^4I_{15/2}$ levels and the Er doping density, respectively and τ_1^* is the measured lifetime of the $^4I_{13/2}$ multiplet in each codoped sample we are considering.

By solving Eqs. 8 in the stationary case, and by substituting in them the expression of the pump rate P, obtained from Eq. 7 as a function of the γ_{Er} parameter, we obtain the inversion parameter γ_{Er-Ce} for Er-Ce codoped crystals as a function of γ_{Er} itself:

#8713 - $15.00 USD Received 15 September 2005; revised 21 October 2005; accepted 21 October 2005

$$\gamma_{Er-Ce} = \frac{\tau_1^* \tau_2^* \, (\beta_{21} + \beta_{Ce}) \, \gamma_{Er}}{\gamma_{Er} \, [\, \tau_1^* \tau_2^* \, (\beta_{21} + \beta_{Ce}) \, - \tau_1 \tau_2 \beta_{21} \,] \, + \, \tau_1 \tau_2 \beta_{21}} \tag{10}$$

This allows to compare, for fixed pump power (i.e., for a given γ_{Er} value), the inversion efficiency as a function of the Ce codoping. In the calculations, we used the 0.35 value of the branching ratio β_{21}, given in [20]. In Fig. 9 the $\gamma_{Er-Ce}/\gamma_{Er}$ ratios in the various samples are compared as a function of γ_{Er} parameter. For clarity reasons we did not show in the Fig. 9 the case of the sample codoped with 0.5% Ce because its behavior is almost undistinguishable from that of the sample codoped with 0.2% Ce. In the same Fig. 9 we depicted also the γ_{Er} parameter itself (horizontal black line), to better compare the values obtained in Ce codoped samples. We can observe a monotonic increase of the inversion parameter for fixed pump level as the Ce concentration is increased. The effect is most striking for the sample with the highest Ce concentration, where $\gamma_{Er-Ce}/\gamma_{Er}$ is about 50% larger than 1 for $\gamma_{Er} = 0.2$, and 33% higher for $\gamma_{Er} = 0.4$.

These results are interesting to give a quantitative evaluation of the Ce effect, even if they have been obtained from a simplified model which neglects upconversion. We have to notice that our model has some approximations that are bigger for crystals with the lowest Ce concentrations and in particular for the crystal doped only with Er, because in this system the upconversion processes are the largest. However, three facts have to be considered: the first one is that the γ_{Er} parameter we obtain from our model is an upper limit for the inversion coefficient we would have if we also consider upconversion. In other words: our model *overestimates* γ_{Er} for a given pump level. The second fact is that in our crystals the Erbium concentrations are the same (within the resolution of our apparatus), and moreover, all the crystals have been compared *at fixed pump rate*: therefore it seems reasonable to expect upconversion to play a similar role in all the samples, but for the effect of Cerium. The last consideration, in fact, is that in Ce-codoped crystals the upconversion processes are strongly reduced, and this is mostly true the highest the Ce concentration.

Moreover for the reasons we just spoke about, if we developed a more complete model by taking into account the upconversion processes, probably we would have obtained a difference in the inversion coefficients between the 4%-Ce doped sample and the solely-Er doped one even larger than the 50% increasing we obtained with our simple model. However, our goal was not to perform a detailed analysis of the Er-Ce energy transfer dynamics, but just to demonstrate the Ce usefulness in improving the feeding of the $^4I_{13/2}$ Er multiplet and therefore in reducing the threshold and increasing the efficiency of a 1.5 μm Er:BaYF laser.

6. Conclusions

In this work the effect of Cerium codoping on Er:BaYF crystals has been investigated. Owing to the intrinsic difficulty to dope BaYF with high concentrations of Cerium, the maximum obtainable Ce concentration was 4% in the melt. However, the results of our investigations show that the Ce presence triggers some cross-relaxation mechanisms from the upper lying manifolds that strongly help the population inversion efficiency for the 1.5 μm emission, without greatly affecting the $^4I_{13/2}$ level lifetime. In particular, by shortening the $^4I_{11/2}$ pumping level decaytime, Ce dramatically decreases both the probabilities of parasitic radiative $^4I_{11/2} \rightarrow {}^4I_{13/2}$ 3 μm transition and upconversion population of the green-emitting level $^4S_{3/2}$. As for the 3 μm transition, it is important to notice that in solely-Er doped crystals, very often this is the preferred lasing channel. Severe suppression of this radiative transition is the only way to obtain laser action at

#8713 - $15.00 USD Received 15 September 2005; revised 21 October 2005; accepted 21 October 2005

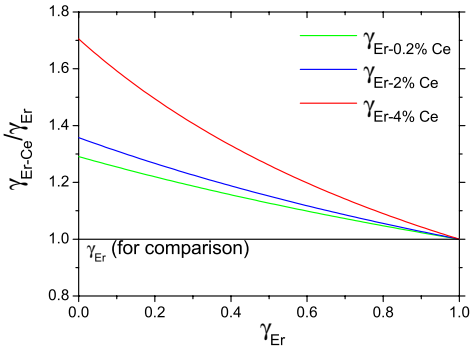

Fig. 9. Comparison of the ratio between the inversion coefficients $\gamma_{Er-Ce}/\gamma_{Er}$ in codoped samples and the inversion coefficient γ_{Er} in the solely-Er doped one for the same pump level.

1.5 μm in such hosts. Regarding the green loss channel, we have to keep in mind that unlike oxides, in fluorides the $^4I_{11/2}$ lifetime is long enough to produce a meaningful parasitic upconversion population of the high-lying levels in the case of 980 nm pumping, with consequent reduction of the pump efficiency. So, it is reasonable to expect that in fluorides the Ce beneficial effect could be even greater than in already studied oxide hosts, and therefore the Cerium addition to Er:BaYF appears very interesting to obtain a low-threshold, high-efficiency 1.5 μm laser.

Acknowledgements

The authors wish to thank Ilaria Grassini for skill and competence in preparing the samples.

#8713 - $15.00 USD Received 15 September 2005; revised 21 October 2005; accepted 21 October 2005